Rigorous verification of chaos in a molecular model

Thomas Rage*
Fakultät für Physik, Albert-Ludwigs-Universität Freiburg, Hermann-Herder-Straße 3, D-79104 Freiburg, Germany

Arnold Neumaier†
Institut für Angewandte Mathematik, Albert-Ludwigs-Universität Freiburg, Hermann-Herder-Straße 10, D-79104 Freiburg, Germany

Christoph Schlier‡
Fakultät für Physik, Albert-Ludwigs-Universität Freiburg, Hermann-Herder-Straße 3, D-79104 Freiburg, Germany
(Received 18 February 1994)

The Thiele-Wilson system, a simple model of a linear, triatomic molecule, has been studied extensively in the past. The system exhibits complex molecular dynamics including dissociation, periodic trajectories, and bifurcations. In addition, it has for a long time been suspected to be chaotic, but this has never been proved with mathematical rigor. In this paper, we present numerical results that, using interval methods, rigorously verify the existence of transversal homoclinic points in a Poincaré map of this system. By a theorem of Smale, the existence of transversal homoclinic points in a map rigorously proves its mixing property, i.e., the chaoticity of the system.

PACS number(s): 05.45.+b, 02.70.Rw, 34.30.+h

I. INTRODUCTION

Since the invention of modern computers, numerical methods provide a useful tool to study the properties of dynamical systems. The entire theory of chaos in dynamical systems would probably not have been invented without the possibility to explore orbits and trajectories of nonlinear dynamical systems through a numerical solution of the underlying equations of motion.

However, due to rounding and truncation errors, the results of numerical studies are in general not exact, but only approximate the true solutions. Especially for chaotic systems (which exhibit an extreme sensitivity of the solutions of the equations of motion with respect to the initial value), the slightest numerical error may cause numerically calculated solutions to be completely wrong and useless. Consequently, when the chaoticity of a dynamical system is to be proved rigorously through numerical studies, one must pay close attention to the question of the reliability of the computed results.

Interval analysis is a branch of mathematics that provides a very elegant way to obtain numerical results with proven reliability. When one adopts the methods of interval analysis appropriately, the obtained results rigorously enclose the exact solution in a box. If a certain property can be shown to hold for all points inside the box, this property must also be true for the exact solution. As a mathematical theory, interval analysis is based on definitions, lemmas, theorems, and their proofs. The interested reader is referred to Moore [1] (elementary) and Neumaier [2] (advanced) for an introduction to interval analysis. The present paper extends the technique of Neumaier and Rage [3], designed for applications to discrete dynamical systems, to a simple continuous-time dynamical system, the so-called Thiele-Wilson system, which has often been used as a model for a collinear triatomic molecule.

Specifically we prove with mathematical rigor that a Poincaré map of this system contains at least one homoclinic fixed point. From its existence it follows that the phase space of this system is mixing (the Smale-Birkhoff theorem; cf. [12], p. 252). This property is generally taken as a definition of "local" or "topological" or "soft" chaos of the system. In contrast to "hard" chaos, such a system also contains regular regions (cf. Figs. 3 and 4), whose size can vary depending on energy and system parameters, but which cannot be determined by the method used here for the proof.

In Sec. II we briefly discuss the Thiele-Wilson system. We introduce Poincaré maps of this system in Sec. III and explain in Sec. IV the chaos criterion that we attempt to verify for a specific Poincaré map. Section V provides a short discussion of the interval techniques we use to rigorously implement this chaos criterion into a computer-assisted proof. Finally, we present in Sec. VI the numerical results that verify the chaos criterion for the Thiele-Wilson system. We end with a short discussion in Sec. VII.

II. THE THIELE-WILSON SYSTEM

Consider a collinear, triatomic molecule in the absence of external forces and molecular rotation (i.e., total ener-

*Present address: Department of Physics, University of Oslo, P.O. Box 1048 Blindern, N-0316 Oslo, Norway.
†Present address: Institüt für Mathematik, Universität Wien, Strüdlhofgasse 4, A-1090 Wien, Austria.
‡Author to whom correspondence should be addressed.

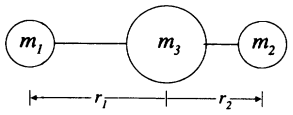

FIG. 1. A schematic sketch of the collinear, triatomic molecule.

gy, center of mass, and total momentum are conserved, and the latter is zero). The geometry of the model is shown in Fig. 1. In terms of the internal coordinates r_i ($i=1,2$) and their canonical conjugate momenta p_i, the Hamiltonian $H(r_i,p_i)$ of this system has the form

$$H=\frac{m_1+m_3}{2m_1m_3}p_1^2+\frac{m_2+m_3}{2m_2m_3}p_2^2-\frac{1}{m_3}p_1p_2+V(r_1,r_2)\ . \tag{1}$$

The Thiele-Wilson (or Double Morse) system is obtained by choosing $m_1=m_2$ for the outer atom masses and taking the potential energy V to be a sum of two equal Morse potentials between adjacent atoms, viz.,

$$V(r_1,r_2)=V_1(r_1)+V_2(r_2)+D\ , \tag{2}$$

with

$$V_i(r)=De^{\beta(r_0-r)}(e^{\beta(r_0-r)}-2)\ . \tag{3}$$

This model was introduced by Thiele and Wilson [4] in 1961 and has been studied repeatedly, e.g., in [5–10]. A common choice of the system parameters (which we adopt) is

$$m_1=m_2=m_3=1.660\,54\times10^{-27}\ \text{kg}\ (=1\ \text{u})\ , \tag{4}$$

$$D=4.746\,15\ \text{eV}\ , \tag{5}$$

$$\beta=1.974\times10^{10}\ \text{m}^{-1}\ , \tag{6}$$

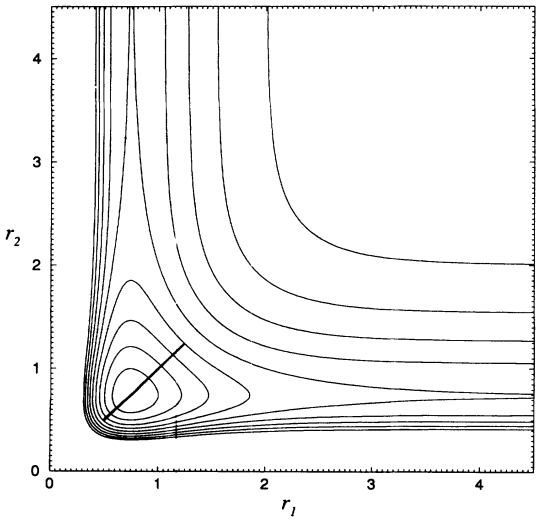

FIG. 2. Equipotential lines of the double Morse well for integer energies between -4 and 4 eV. The symmetric stretch at $E=-1$ eV is shown as a thick line.

$$r_0=0.741\,27\times10^{-10}\ \text{m}\ . \tag{7}$$

With these values, the model approximates a collinear H_3^+ system in its electronic ground state quite well. Figure 2 shows equipotential lines of this system for integer energies between -4 and 4 eV. Notice that the energy scale in (2) is chosen such that the first dissociation limit is at energy $E=0$ eV. In the following we always consider this system at the energy $E=-1$ eV. The thick line in Fig. 2 corresponds to a simple periodic trajectory, called the symmetric stretch of this system at this energy. The period T of this trajectory is approximately $T=13.5208$ fs.

III. POINCARÉ MAPS

To define a general Poincaré map in our system, we perform a linear transformation of coordinates $(r_1,r_2)\rightarrow(x_1,x_2)$ through

$$\begin{aligned} x_1&:=\begin{bmatrix} n_1 \\ n_2 \end{bmatrix}\begin{bmatrix} r_1 & -a_1 \\ r_2 & -a_2 \end{bmatrix} \\ x_2&:=\begin{bmatrix} -n_2 \\ n_1 \end{bmatrix}\begin{bmatrix} r_1 & -a_1 \\ r_2 & -a_2 \end{bmatrix}\ , \end{aligned} \tag{8}$$

where (n_1,n_2) is the normal vector and (a_1,a_2) a particular point of a line called *surface of section* in (r_1,r_2) space. The momentum variables x_3 and x_4 are chosen canonically conjugate to x_1 and x_2, respectively. In terms of these Poincaré coordinates $x=(x_1,x_2,x_3,x_4)$, Hamilton's equations of motion,

$$\dot{x}_1=\frac{\partial H}{\partial x_3}\ ,\ \dot{x}_2=\frac{\partial H}{\partial x_4}\ ,\ \dot{x}_3=-\frac{\partial H}{\partial x_1}\ ,\ \dot{x}_4=-\frac{\partial H}{\partial x_2}\ , \tag{9}$$

define a system of ordinary differential equations of the form $\dot{x}=g(x)$.

The Poincaré map of some trajectory $x(t)$ is obtained by integrating this system from an initial value x^0 at $t=0$, and tracing out the sequence $(x_1(t_j),x_3(t_j))$ of points at times t_j at which $x_2(t_j)=0$ and $x_4(t_j)>0$. One can show that this procedure defines a two-dimensional, area conserving, invertible map F_E: $\mathbb{D}\subseteq\mathbb{R}^2\rightarrow\mathbb{D}$ through

$$F_E(x_1(t_j),x_3(t_j)):=(x_1(t_{j+1}),x_3(t_{j+1}))\ , \tag{10}$$

which is called the Poincaré map. The index E on F expresses the fact that—for a given surface of section—the map does only depend on the (conserved) system energy $E=H(x)$, which can be considered as a continuous parameter. Note that a periodic trajectory produces a periodic orbit in any Poincaré map of the system, and that the stability type of the orbit will be the same as the stability type of the trajectory. Thus, Poincaré maps reduce our problem of studying a four-dimensional flow to the study of a family of two-dimensional maps.

Figure 3 shows an approximate phase portrait of a typical Poincaré map of the Thiele-Wilson system for

$$n_1=n_2=1\ \text{m}^{-1},\ a_1=a_2=0.8\times10^{-10}\ \text{m}\ .$$

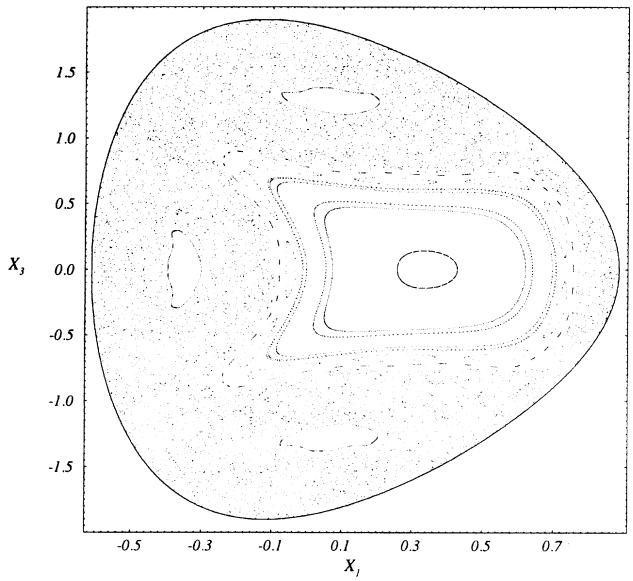

FIG. 3. Phase portrait of a typical Poincaré map of the Thiele-Wilson system ($E=-1$ eV, $n_1=n_2=1$ m^{-1}, $a_1=a_2=0.8\times10^{-10}$ m).

To create this picture, 500 iterates of 10 different suitably chosen starting points (x_1^0,x_3^0) were calculated approximately by numerical integration of the corresponding initial value problem:

$$\dot{x}(t)=g(x(t))\ ,\quad x(t=0)=x^0\ , \tag{11}$$

using a Gear-Hybrid integration routine. An interactive FORTRAN program to produce and analyze phase portraits of Poincaré maps of the Thiele-Wilson system was provided by Seiter [11]. We do not discuss the details of this picture, but only state that it shows a very regular pattern, which can be described as hierarchy of islands. The interested reader is referred to the textbooks of Guckenheimer and Holmes [12] or Tabor [13] for a general discussion of the dynamics of nonlinear dynamical systems.

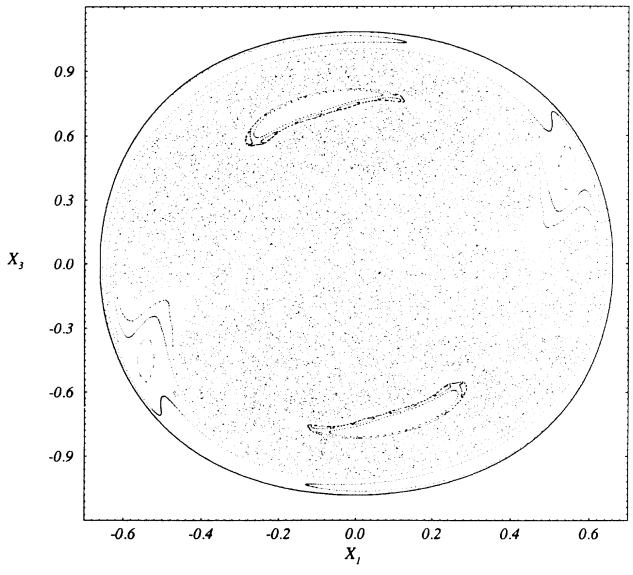

FIG. 4. Phase portrait of a Poincaré map of the Thiele-Wilson system ($E=-1$ eV, $n_1=-n_2=1$ m^{-1}, $a_1=a_2=0.8\times10^{-10}$ m).

Figure 4 shows a phase portrait of a Poincaré map with a different surface of section. In contrast to Fig. 3, this picture exhibits much less regular patterns but most points seem to be scattered quite randomly in the plane. Phase portraits like those of Figs. 3 and 4 are usually interpreted as a proof of chaos in the system. However, since we want to establish here a mathematically rigorous proof of chaos, we have to use a precise criterion for chaos, which we take from Smale [14].

IV. THE CHAOS CRITERION

We briefly discuss the chaos criterion that we attempt to prove for the Poincaré map shown in Fig. 4. More extensive discussions can again be found in Refs. [12] or [13].

For any fixed point x^* of a invertible map F with inverse F^{-1}, its *stable* and *unstable sets* $W^s(x^*)$ and $W^u(x^*)$ are defined through

$$W^s(x^*):=\{x\in\Omega|\lim_{n\to\infty}F^n(x)=x^*\} \tag{12}$$

and

$$W^u(x^*):=\{x\in\Omega|\lim_{n\to\infty}F^{-n}(x)=x^*\}\ , \tag{13}$$

respectively. These sets are nonempty, invariant under F, and—in the case of an area preserving map—form manifolds of $\mathbb{D}$ (cf. Smale [14]).

The symmetric stretch of the Thiele-Wilson system is (at most system energies) an unstable trajectory that produces a hyperbolic fixed point $x^*=(x_1^*,x_3^*)=(0,0)$ in those Poincaré maps for which the surface of section satisfies $n_1=-n_2$ and $a_1=a_2$. Through a careful choice of starting points (analogous to the description in [3]), parts of the two manifolds of the hyperbolic fixed point $x^*=(0,0)$ were traced out in Fig. 5. One clearly sees the hyperbolic fixed point in the center of the picture, marked through a transversal crossing of the two manifolds.

Note that, close to the fixed point x^*, the two manifolds look almost linear. This illustrates the observation that close to a fixed point x^* any map F is well approximated by the linear mapping

$$\tilde{F}(x)=x^*+F'(x^*)(x-x^*)\ .$$

The matrix $F'(x^*)$, the *Jacobian* of F at x^*, is defined by

$$F'_{ij}(x^*)=\frac{\partial F_i(x^*)}{\partial x_j}\ . \tag{14}$$

Figure 5 suggests that there exist transversal intersections of the two manifolds distinct from the fixed point; any such intersection point is called a *transversal homoclinic point.* It is a result of Smale [14] that a conservative map containing at least one transversal homoclinic point is a mixing system, and therefore (by definition)

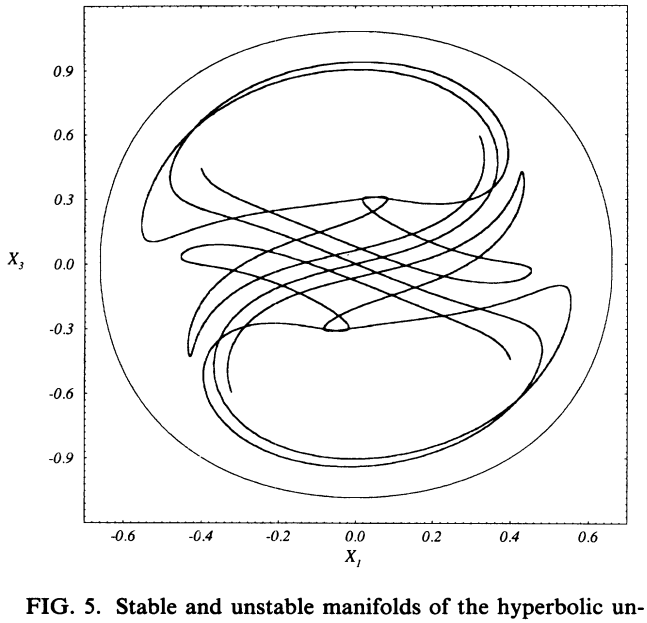

FIG. 5. Stable and unstable manifolds of the hyperbolic unstable fixed point of the Poincaré map of Fig. 4.

chaotic at least in the vicinity of the hyperbolic fixed point. Consequently, if Fig. 5 was an exact picture, i.e., if the two lines would exactly show parts of the manifolds of the fixed point, it would be a sufficient proof of the chaoticity of the Thiele-Wilson system.

However, the two lines were constructed by connecting some points that were calculated via an approximate method to solve the equation of motion of the system. Figure 5 therefore give us only (at best) an approximate picture of the manifolds of the system, and—from the point of view of a mathematician—cannot serve as a proof of anything.

V. INTERVAL TECHNIQUES

In the following, we describe a strategy to rigorously prove the existence of one of the transversal homoclinic points that are present in Fig. 5. To do so, we first recall some basic definitions of interval analysis: (i) An *interval* x is defined as a closed subset of the real line $\mathbb{R}$; (ii) an *interval vector* is a vector with interval components, and an *interval matrix* is a matrix with interval entries; (iii) with $F: \mathbb{D}\subset\mathbb{R}^n\rightarrow\mathbb{R}^m$ being a function, an *interval enclosure* y of the image $F(x)$ of an interval (vector) x is an interval (vector) that satisfies

$$F(\tilde{x})\in y \quad \text{for all } \tilde{x}\in x \ ; \tag{15}$$

and (iv) with F' being the Jacobian of a function F, an interval enclosure Y of the Jacobian $F'(x)$ of an interval (vector) x is an interval (matrix) that satisfies

$$F'(\tilde{x})\in Y \quad \text{for all } \tilde{x}\in x \ . \tag{16}$$

Additionally, we introduce the term *linear enclosure:* Consider a curve $x(t)$ (e.g., a trajectory or a manifold) that is parametrized through the parameter t. A local representation of $x(t)$ is given through a point $x(t_0)$ of the curve and the tangent vector $K(x(t_0))$ of the curve at $x(t_0)$. In a similar way, a local enclosure of the curve inside an interval vector is established through an interval Σ and interval vectors Ω, x_0, and K such that

(i) for any $t\in\Sigma$, the corresponding point $x(t)$ is contained in Ω; (ii) for any $t\in\Sigma$, the tangent vector of the curve at the point $x(t)$ is contained in K; and (iii) at least for one $t_0\in\Sigma$, the interval vector x_0 encloses the point $x(t_0)$ of the curve.

We call such a local enclosure of a curve a linear enclosure and use the shorthand notation $x(t)\in\{\Omega,\Sigma,x_0,K\}$. A graphical representation of a linear enclosure of a two-dimensional curve is contained in [3].

A. Rigorous verification of transversal homoclinic points

A complete discussion of the mathematical background and computer implementation of this method together with its application to Chirikov's standard map is given in Neumaier and Rage [3]. Here, we briefly explain the main steps of the underlying strategy. To ease the formulation, let $W^s(t)$ $[W^u(t)]$ denote parametrizations of the stable [unstable] manifold of the hyperbolic fixed point, respectively. These parametrizations are chosen such that $W^s(0)$ and $W^u(0)$ both describe the hyperbolic fixed point.

In a first step, one has to verify rigorously the existence of a hyperbolic fixed point x^* of the map and to construct a narrow interval enclosure of it. Next, one constructs linear enclosures $\{\Omega^{s/u},x^*,\Sigma^{s/u},K^{s/u}\}$ of the two manifolds $W^{s/u}$ of the hyperbolic fixed point for some narrow intervals $\Omega^{s/u}$ that enclose x^*. This is done through the construction of appropriate intervals $\Sigma^{s/u}$ and $K^{s/u}$ from the calculation of $F'(\Omega^s)$ and $F'^{-1}(\Omega^u)$.

By choosing special values for the four parameters $t_0^{s/u}$ and $\delta^{s/u}$, and with

$$x_u^{s/u}:=x^*+K^{s/u}t_0^{s/u} \ , \tag{17}$$

one defines linear enclosures $\{\Omega^{s/u},x_0^{s/u},[-\delta^{s/u},\delta^{s/u}],K^{s/u}\}$ that select small pieces of the linear enclosures $\{\Omega^{s/u},x^*,\Sigma^{s/u},K^{s/u}\}$. As the two manifolds are invariant under F and F^{-1}, these small pieces can be iterated $N^{s/u}$ times along the trajectory, giving linear enclosures $\{\Gamma^{s/u},y_0^{s/u},[-\delta^{s/u},\delta^{s/u}],H^{s/u}\}$ of the two manifolds in the neighborhood of a suspected transversal homoclinic point of the map. In practice, one calculates these iterated linear enclosures from

$$y_0^s\supseteq(F^{-1})^{N^s}(x_0^s) \ , \quad H^s\supseteq(F'^{-1})^{N^s}(x_e^s) \ , \tag{18}$$

$$y_0^u\supseteq F^{N^u}(x_0^u) \ , \quad H^u\supseteq(F')^{N^u}(x_e^u) \ , \tag{19}$$

where

$$x_e^{s/u}:=x_0^{s/u}+K^{s/u}[-\delta^{s/u},\delta^{s/u}] \ . \tag{20}$$

From the solution (x_h,d^s,d^u) of the system of linear interval equations,

$$\begin{bmatrix} I & -H^s & 0 \\ I & 0 & -H^u \end{bmatrix} \begin{bmatrix} x_h \\ d^s \\ d^u \end{bmatrix} = \begin{bmatrix} y_0^s \\ y_0^u \end{bmatrix}, \tag{21}$$

a rigorous verification of transversal intersection of the two manifolds is obtained if

$$d^{s/u} \subset [-\delta^{s/u}, \delta^{s/u}] . \tag{22}$$

In this case, x_h is a valid enclosure of the corresponding transversal homoclinic point, and the chaos proof is perfect.

We note that the chances of a successful chaos proof depend crucially on a good choice of the iteration numbers $N^{s/u}$ as well as the parameters $t_0^{s/u}$, and $\delta^{s/u}$, as explained in [3]. If this is not done carefully, the enclosure (22) will not hold, and no conclusion can be drawn. Of course, if no homoclinic point exists in a neighborhood of the suspected point, (22) will be violated no matter how the parameters are chosen.

B. Interval enclosures for Poincaré maps

Our strategy to enclose transversal homoclinic points is based on the possibility to calculate narrow interval enclosures for $F(x)$ and $F'(x)$ of a given mapping F for any interval x. Several methods to calculate such interval enclosures for explicit functions are discussed in [2]. In the case of a Poincaré map F_E of the Thiele-Wilson system (an implicit function), we can construct interval enclosures of $F_E(x_1^0, x_3^0)$ for any interval (x_1^0, x_3^0) through an *interval integration* of the corresponding initial value problem. An appropriate method to calculate interval enclosures of the solution of an initial value problem (with interval initial value) for a series of equidistant time points $t_n = nh$ $(n = 0, 1, \ldots)$ was developed by Lohner [15]. With the help of such a program, interval enclosures of $F_E(x_1^0, x_3^0)$ are established in the following way.

For a given interval vector (x_1^0, x_3^0), we construct a complete initial interval for the integration by setting $x_2^0 = 0$ and calculating x_4^0 as the interval enclosure of the set $u(x_1^0, x_2^0, x_3^0, E)$, where the function u is defined by $H(x_1, x_2, x_3, u) = E$ and $H(x)$ is the Hamiltonian of the system in terms of the Poincaré coordinates x.

We then integrate the initial value problem, obtaining interval vectors $x(t_j)$ until we find a time point t_j such that

$$\max x_2(t_j) < 0 , \quad \min x_4(t_j) > 0 , \tag{23}$$

$$\min x_2(t_{j+1}) > 0 , \quad \min x_4(t_{j+1}) > 0 . \tag{24}$$

By continuity, there is a time $t \in [t_j, t_{j+1}]$ such that the trajectory $x(t)$ satisfies $x_2(t) = 0$, $x_4(t) > 0$. To improve the accuracy, we restart the integration with a smaller steplength from the initial value $x(t_j)$. As a result, we obtain two new numbers j_1 and j_2 such that

$$\max x_2(t_{j_1}) < 0 , \quad \min x_4(t_{j_1}) > 0 , \tag{25}$$

$$\min x_2(t_{j_2}) > 0 , \quad \min x_4(t_{j_2}) > 0 . \tag{26}$$

From this we conclude that with

$$y_1^0 := \bigcup_{i=j_1}^{j_2} x_1(t_i) , \quad y_3^0 := \bigcup_{i=j_1}^{j_2} x_3(t_i) , \tag{27}$$

the interval (y_1^0, y_3^0) is an interval enclosure of $F(x_1^0, x_3^0)$.

The construction of interval enclosures of F' for a given interval x is performed in a similar way using

$$M_{ij}(t) = \frac{\partial x_i(t)}{\partial x_j(0)} \quad \text{and} \quad L_{ij}(x) = \frac{\partial g_i(x)}{\partial x_j} . \tag{28}$$

Here $L(x)$ is known and $M(t)$ can be found from an interval integration of the *extended* initial value problem:

$$\dot{x}(t) = g(x(t)) , \quad \dot{M}(t) = L(x(t)) M(t) , \tag{29}$$

with initial values $x(t=0) = x^0$ and $M(t=0) = 1$, the 4×4 unity matrix. With these definitions, we find that at some time point t_j with $x_2(t_j) = 0$ and $x_4(t_j) > 0$, we have

$$\begin{bmatrix} F'_{11}(x_1^0, x_3^0) & F'_{12}(x_1^0, x_3^0) \\ F'_{21}(x_1^0, x_3^0) & F'_{22}(x_1^0, x_3^0) \end{bmatrix} = \begin{bmatrix} M_{11}(t_j) & M_{13}(t_j) \\ M_{31}(t_j) & M_{33}(t_j) \end{bmatrix} . \tag{30}$$

VI. NUMERICAL RESULTS

In this section we present the numerical results that lead to a rigorous verification of chaos in the Thiele-Wilson system. All interval calculations were performed on a IBM 3090-180 computer where the programming package ACRITH-XSC [16] was available to us. An ACRITH version of the AWA program for the interval enclosure of initial value problems, described in Lohner [15], was provided by this author, and some special ACRITH programs (implementing the ideas described in [3] and in Sec. V) were written by us.

The numerical calculation of interval enclosures of F and F' of a Poincaré map with the AWA program is a very CPU time consuming procedure. With reasonable choices of the step size and order parameters of the AWA program, the performance of only one time step $t_n \to t_{n+1}$ of the interval integration of the initial value problem took about 8.5 sec machine time. To compute one iteration of the mapping F_E took about 2 h machine time. The computation of the derivative F'_E is even more time consuming and took about 8 h machine time. To perform all the calculations necessary to rigorously enclose a transversal homoclinic point—including all unsuccessful trial calculations—took us about six months real time and used about 2000 h CPU time. However, this slowness seems to be mainly due to the implementations of the interval arithmetic and of the version of the AWA program available to us, and not to the inherent complexity of the enclosure problem.

In the presentation of our results, we follow the notation of [3] in order to allow for a comparison with the detailed discussion therein. Thus from now on, the variable t no longer denotes time, but rather the variable parametrizing the manifolds. We concentrate on the Poincaré map characterized by the choice (cf. Fig. 5).

$$E=-1\ \text{eV}\ ,$$
$$n_1=-n_2=1\ \text{m}^{-1}\ , \tag{31}$$
$$a_1=a_2=0.8\times10^{-10}\ \text{m}\ .$$

This map has a fixed point at $x^*=(0,0)$ which corresponds to the symmetric stretch of the Thiele-Wilson system. From the calculation of an interval enclosure of $F'(\Omega^s)$ for the box

$$\Omega^s=\begin{bmatrix}[0,2.605\times10^{-8}]\\ [0,1.139\times10^{-8}]\end{bmatrix}\ , \tag{32}$$

we obtain a linear enclosure of the stable manifold $W^s(x^*)$ in Ω^s with the help of Theorem 1 in [3]. This linear enclosure is characterized by the outward rounded values

$$K^s\subseteq\begin{bmatrix}[0.916\,280\,03,0.916\,281\,10]\\ [0.400\,536\,67,0.400\,537\,44]\end{bmatrix}\ , \tag{33}$$

$$\Sigma^s\subseteq[0,2.843\,017\,33\times10^{-8}] \tag{34}$$

for the intervals K^s and Σ^s. Similarly, putting

$$\Omega^u=\begin{bmatrix}[0,2.068\times10^{-8}]\\ [-1.489\times10^{-8},0]\end{bmatrix} \tag{35}$$

and calculating $F'^{-1}(\Omega^u)$, we obtain a linear enclosure of the unstable manifold $W^u(x^*)$ with the outward rounded intervals

$$K^u\subseteq\begin{bmatrix}[0.811\,566\,39,0.811\,567\,859]\\ [-0.584\,259\,51,-0.584\,258\,867]\end{bmatrix}\ , \tag{36}$$

$$\Sigma^u\subseteq[0,2.548\,158\,74\times10^{-8}]\ . \tag{37}$$

Taking the free parameters of the method (cf. [3]) to be

$$t_0^s=2.584\,635\,1\times10^{-8},\quad \delta^s=2\times10^{-13}\ ,\quad N^s=10\ , \tag{38}$$

$$t_0^u=2.315\,970\,4\times10^{-8},\quad \delta^u=4\times10^{-13}\ ,\quad N^u=9\ , \tag{39}$$

we transform pieces of these two linear enclosures into the neighborhood of the suspected homoclinic point near

$$(x_1,x_3)=(-0.32,0.21)$$

(cf. Fig. 5), in order to obtain linear enclosures of the stable and unstable manifolds in the neighborhood of this point. The calculations lead to the outward rounded values

$$y_0^s\subseteq\begin{bmatrix}[-0.321\,787\,08,-0.321\,785\,79]\\ [0.207\,505\,33,0.207\,505\,87]\end{bmatrix}\ , \tag{40}$$

$$H^s\subseteq\begin{bmatrix}[3.390\,202\,18\times10^7,3.391\,230\,21\times10^7]\\ [1.372\,892\,31\times10^7,1.374\,008\,00\times10^7]\end{bmatrix}\ , \tag{41}$$

$$y_0^u\subseteq\begin{bmatrix}[-0.321\,786\,70,-0.321\,786\,34]\\ [0.207\,505\,48,0.207\,505\,68]\end{bmatrix}\ , \tag{42}$$

$$H^u\subseteq\begin{bmatrix}-1.102\,819\,59\times10^7,-1.102\,719\,37\times10^7]\\ [5.834\,074\,79\times10^6,5.835\,086\,63\times10^6]\end{bmatrix} \tag{43}$$

for the intervals that characterize the iterated linear enclosures. Finally, the solution of the system of linear interval equations reads

$$x_h\subseteq\begin{bmatrix}[-0.321\,787\,27,-0.321\,785\,74]\\ [0.207\,505\,19,0.207\,505\,95]\end{bmatrix}\ , \tag{44}$$

$$d^s\subseteq[-2.683\,716\,99\times10^{-14},2.294\,334\,64\times10^{-14}]\ , \tag{45}$$

$$d^u\subseteq[-6.851\,187\,00\times10^{-14},6.494\,458\,38\times10^{-14}]\ . \tag{46}$$

We conclude from $d^{s/u}\subset[-\delta^{s/u},\delta^{s/u}]$ that x_h is an interval enclosure of a transversal homoclinic point of the map, proving the Thiele-Wilson system to be chaotic.

VII. CONCLUSIONS

A Poincaré map like that of Fig. 3 will normally convince a physicist that a dynamical system is chaotic, though this is no proof whatsoever. Further confirmation can be obtained by showing—by standard numerical integration with approximate error control—the existence of an unstable fixed point of the system under discussion plus one homoclinic point, as Berblinger and Schlier [5] have done for the Thiele-Wilson system. No physicist will doubt such a proof of chaos.

But if one wants mathematical rigor, one must additionally believe that some shadow theorem is applicable, or that *the world is continuous anyhow.* It is therefore gratifying that the implementation of modern interval arithmetic on computers (carefully employing directed rounding and the like) allows one to go one step further, and make such proofs mathematically rigorous. Like other mathematical proofs, only human errors (in the implementation of interval arithmetic, or in the special programs needed for the problem) can make it invalid.

In this paper we have shown for a simple molecular model with two degrees of freedom that such a proof of chaos can indeed be implemented. The techniques used in this and the former paper [3] are quite general, and can be modified easily for other systems. We feel that they are more general than the pioneering chaos proof by Rod, Pecelli, and Churchill [17] for the Henon-Heiles system. Still, it is clear that for the physicist an amount of rigor like that applied here will remain an exception. More generally, however, this example shows that interval methods to establish rigorous numerical proofs are now available to physicists, and may be useful in other fields, too.

ACKNOWLEDGMENTS

We are grateful to Dr. Rudolf Lohner for providing us with an ACRITH version of his program AWA for the calculation of interval enclosures of initial value problems. We thank Ansgar Seiter for his help in producing and analyzing Poincaré maps of the Thiele-Wilson system. The computations were performed on the IBM 3090-180 of the University Computer Center, whose help is also acknowledged.

[1] R. E. Moore, *Methods and Applications of Interval Analysis* (SIAM, Philadelphia, 1979).
[2] A. Neumaier, *Interval Methods for Systems of Equations* (Cambridge University Press, Cambridge, England, 1990).
[3] A. Neumaier and Th. Rage, Physica D **67**, 327 (1993).
[4] E. Thiele and D. J. Wilson, J. Chem. Phys. **35**, 1256 (1961).
[5] M. Berblinger and Ch. Schlier, Chem. Phys. Lett. **145**, 299 (1988).
[6] R. H. Bisseling, R. Kosloff, J. Manz, F. Mrugala, J. Röhlmelt, and G. Weichselhammer, J. Chem. Phys. **86**, 2626 (1987).
[7] P. Brumer and J. W. Duff, J. Chem. Phys. **65**, 3566 (1976).
[8] D. E. Fitz and P. Brumer, J. Chem. Phys. **70**, 5527 (1979).
[9] T. Terasaka and T. Matsushita, Phys. Rev. A **32**, 538 (1985), and references cited therein.
[10] Ch. Schlier, Chem. Phys. **105**, 361 (1986).
[11] A. Seiter, diploma thesis, Freiburg, 1992.
[12] J. Guckenheimer and P. Holmes, *Nonlinear Oszillations, Dynamical Systems, and Bifurcations of Vector Fields* (Springer, Berlin, 1983).
[13] M. Tabor, *Chaos and Integrability in Nonlinear Dynamics* (Wiley, New York, 1989).
[14] S. Smale, Bull. Am. Math. Soc. **73**, 747 (1967).
[15] R. Lohner, in *Computerarithmetic: Scientific Computation and Programming Languages,* edited by E. Kaucher, U. Kulisch, and Ch. Ullrich (Teubner, Stuttgart, 1987), pp. 255–286.
[16] ACRITH–XSC: IBM High Accuracy Arithmetic, Extended Scientific Computation, Version 1, Release 1. General Information, GC 33-6461-01 (IBM Deutschland, Böblingen, 1990).
[17] D. L. Rod, G. Pecelli, and R. C. Churchill, J. Differ. Equations **24**, 329 (1977).

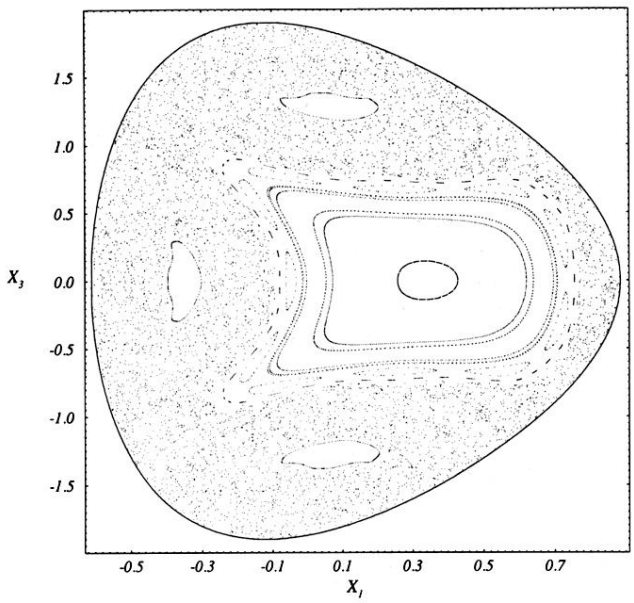

FIG. 3. Phase portrait of a typical Poincaré map of the Thiele-Wilson system ($E=-1$ eV, $n_1=n_2=1$ m^{-1}, $a_1=a_2=0.8\times10^{-10}$ m).

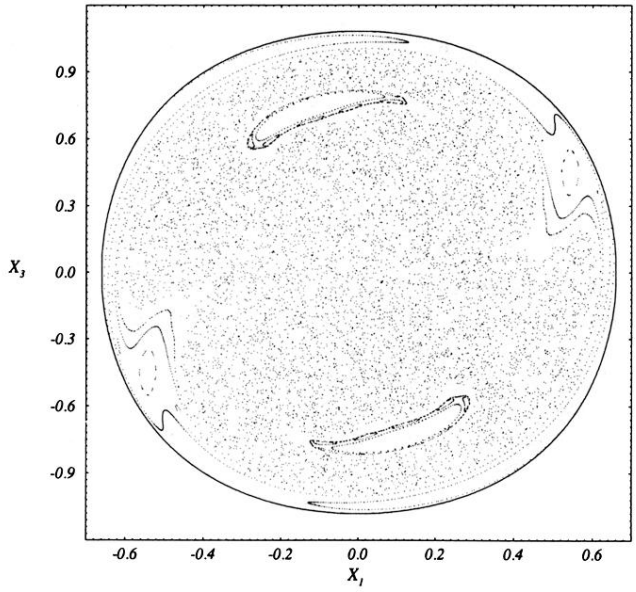

FIG. 4. Phase portrait of a Poincaré map of the Thiele-Wilson system ($E=-1$ eV, $n_1=-n_2=1$ m^{-1}, $a_1=a_2=0.8\times10^{-10}$ m).